REVIEW

Imaging

Neoatherosclerosis: overview of histopathologic findings and implications for intravascular imaging assessment

Fumiyuki Otsuka[1], Robert A. Byrne[2], Kazuyuki Yahagi[1], Hiroyoshi Mori[1], Elena Ladich[1], David R. Fowler[3], Robert Kutys[1], Erion Xhepa[2], Adnan Kastrati[2], Renu Virmani[1], and Michael Joner[1]*

[1]CVPath Institute, Inc., 19 Firstfield Road, Gaithersburg, MD 20878, USA; [2]Deutsches Herzzentrum München, Technische Universitat München, Munich, Germany; and [3]Office of the Chief Medical Examiner, Baltimore, MD, USA

Despite the reduction in late thrombotic events with newer-generation drug-eluting stents (DES), late stent failure remains a concern following stent placement. In-stent neoatherosclerosis has emerged as an important contributing factor to late vascular complications including very late stent thrombosis and late in-stent restenosis. Histologically, neoatherosclerosis is characterized by accumulation of lipid-laden foamy macrophages within the neointima with or without necrotic core formation and/or calcification. The development of neoatherosclerosis may occur in months to years following stent placement, whereas atherosclerosis in native coronary arteries develops over decades. Pathologic and clinical imaging studies have demonstrated that neoatherosclerosis occurs more frequently and at an earlier time point in DES when compared with bare metal stents, and increases with time in both types of implant. Early development of neoatherosclerosis has been identified not only in first-generation DES but also in second-generation DES. The mechanisms underlying the rapid development of neoatherosclerosis remain unknown; however, either absence or abnormal endothelial functional integrity following stent implantation may contribute to this process. In-stent plaque rupture likely accounts for most thrombotic events associated with neoatherosclerosis, while it may also be a substrate of in-stent restenosis as thrombosis may occur either symptomatically or asymptomatically. Intravascular optical coherence tomography is capable of detecting neoatherosclerosis; however, the shortcomings of this modality must be recognized. Future studies should assess the impact of iterations in stent technology and risk factor modification on disease progression. Similarly, refinements in imaging techniques are also warranted that will permit more reliable detection of neoatherosclerosis.

Keywords   Coronary disease • Imaging • Neoatherosclerosis • Pathology • Restenosis • Stents • Thrombosis

Introduction

Coronary artery disease (CAD) remains the leading cause of death worldwide, contributing to over 7.2 million deaths annually.[1,2] The introduction of percutaneous coronary intervention (PCI) revolutionized the treatment of patients with obstructive CAD including those presenting with acute myocardial infarction.[3,4] In addition, the development of drug-eluting stents (DES) successfully targeted the problem of neointimal overgrowth within the stented segment.[5] However, this success came at the cost of a substantial delay in vascular healing due to the potent effects of the released anti-proliferative drugs.[6] Observational studies have shown a steady increase in the cumulative incidence of late and very late stent thrombosis (LST/VLST) following first-generation DES placement.[7–11] However, the evolution of DES technology, particularly the introduction of second-generation DES, has improved patient outcomes by decreasing the risk of late thrombotic events while maintaining anti-restenotic efficacy.[8,12] Nevertheless, late stent failure remains a concern even with the use of contemporary DES since clinical trials have shown an increase in the cumulative incidence of target lesion revascularization with time in all generations of DES.[13–16]

* Corresponding author. Tel: +1 301 208 3570, Fax: +1 301 208 3745, Email: mjoner@cvpath.org; michaeljoner@me.com

While delayed arterial healing characterized by poor strut coverage has been identified as the major pathologic substrate responsible for LST/VLST following first-generation DES placement,[6,17] several other factors are associated with late DES failure, which include hypersensitivity reaction, malapposition with excessive fibrin deposition, stent fracture, and in-stent neoatherosclerosis.[18-20] Early pathological studies showed that the incidence of neoatherosclerosis increased with time and develops earlier and more frequently in first-generation DES when compared with bare metal stents (BMS).[20,21] Our recent human autopsy study confirmed prior randomized and non-randomized clinical trials showing second-generation cobalt-chromium everolimus-eluting stents (CoCr-EES) have a substantially lower prevalence of LST/VLST, with a striking reduction in uncovered struts, less inflammation and fibrin deposition, and a lower prevalence of overall stent fracture when compared with the first-generation DES.[22] Nevertheless, the observed frequency of neoatherosclerosis did not differ significantly between CoCr-EES and first-generation DES.[22] Therefore, the prevalence of neoatherosclerosis remains to be determined with contemporary DES devices. Moreover, its early detection with intravascular imaging modalities in the clinical setting might facilitate targeted therapy to alter its natural history and prevent complications including VLST and late in-stent restenosis.

The current review provides an overview of the histopathology of neoatherosclerosis within BMS and DES and summarizes the observations from pathologic and clinical imaging studies with respect to the prevalence and characteristics of neoatherosclerosis. In addition, the benefits and limitations of contemporary intravascular imaging modalities along with potential strategies to treat and prevent neoatherosclerosis are discussed.

Morphological characteristics of in-stent neoatherosclerosis

In-stent neoatherosclerosis is histologically characterized by an accumulation of lipid-laden foamy macrophages with or without necrotic core formation and/or calcification within the neointima.[20] There is no communication between the lesion within the neointima and the underlying native atherosclerosis. The earliest feature of neoatherosclerosis is foamy macrophage clusters, which is frequently seen either in the peri-strut area (*Figure 1A*) or close to the luminal surface (*Figure 1B*). The accumulation of foamy macrophages may progress to form fibroatheroma, and these may be observed on the luminal surface (*Figure 1C*) or within the deeper neointimal layers (*Figure 1D–F*). The necrotic core generally contains discrete collections of acellular debris with substantial amount of free cholesterol and near complete depletion of extracellular matrix. Occasionally, the necrotic core of neoatherosclerotic plaque shows extensive haemorrhage with fibrin deposition (*Figure 1G* and *H*), which likely originated from the luminal surface through fissure or rupture, although it may also occur from leaky vasa vasorum that originate from the adventitia. Moreover, further infiltration of foamy macrophages within the neointima results in the thinning of the fibrous cap to form thin-cap fibroatheroma (TCFA) (*Figure 1I* and *J*), which may lead to in-stent plaque rupture.

Calcification can also be seen within the neointima especially in implants with relatively long duration of follow-up. Morphological

characteristics vary widely from microcalcification (*Figure 1D*) to fragmented or sheet calcification (*Figure 1H* and *K*). The process of calcification is complex; however, it is conceivable that microcalcification can be attributed to apoptosis of foamy macrophages or smooth muscle cells similar to that observed in native disease, whereas fragmented or sheets of calcification are likely derived from calcification of the collagen, extracellular matrix, and smooth muscle cells.[23] What is unique in neoatherosclerosis of DES is calcification of fibrin. In particular, in our experience, calcification of fibrin is frequently observed in paclitaxel-eluting stents (PES; TAXUS Express or TAXUS Liberté, Boston Scientific, Natick, MA, USA) (*Figure 1L*).

Potential mechanisms of accelerated neoatherosclerosis

While atherosclerosis in native coronary arteries develops over decades, in-stent neoatherosclerosis seems to occur in months to years following stent placement and rapidly and more frequently in DES when compared with BMS.[20,22] The mechanisms responsible for the accelerated atherosclerosis in stented segments, particularly in DES, remain unknown to date; however, it is speculated that incompetent and dysfunctional endothelial coverage of the stented segment contributes to this process. Stent implantation causes vascular injury with endothelial denudation. Incomplete maturation of the regenerated endothelium, which is characterized by poor cell-to-cell junctions, reduced expression of anti-thrombotic molecules, and decreased nitric oxide production, are more frequently observed in DES when compared with BMS; this is likely associated with the anti-proliferative effects of the eluted drugs.[24-27] Poorly formed cell junctions underlie impaired barrier function of the endothelium, which allows greater amount of lipoproteins to enter the sub-endothelial space, leading to the development of neoatherosclerosis (*Figure 2A*). In support of this, in rabbit iliac arteries, the expression of platelet endothelial cell adhesion molecule-1 (PECAM-1), a transmembrane protein, was greater in CoCr-EES when compared with sirolimus-eluting stent (SES; Cypher, Cordis Corp., Miami Lakes, FL, USA), PES, and endeavor zotarolimus-eluting stents (E-ZES; Medtronic, Santa Rosa, CA, USA) at 14 days following stent implantation; however, all DES showed decreased expression of PECAM-1 and anti-thrombotic co-factor thrombomodulin when compared with BMS.[24] Accelerated neoatherosclerosis after DES is likely a direct consequence of delayed vascular healing, although a continuous correlation of its magnitude with the degree of delayed vascular healing cannot be concluded to date. This may account for the comparable prevalence of neoatherosclerosis between CoCr-EES and first-generation DES: although healing seems improved with CoCr-EES, endothelial maturation may be still insufficient in CoCr-EES when compared with BMS.[24] Also, BMS develop atherosclerosis earlier than do native arteries, suggesting that mechanisms other than the involvement of anti-proliferative drug may be associated with incompetent endothelium within the stented segment.

Stent placement causes local blood flow disturbances associated with complex spatiotemporal changes in shear stress. It is likely that blood flow disturbances following stent implantation contribute to activation of regenerating endothelial cells to promote the
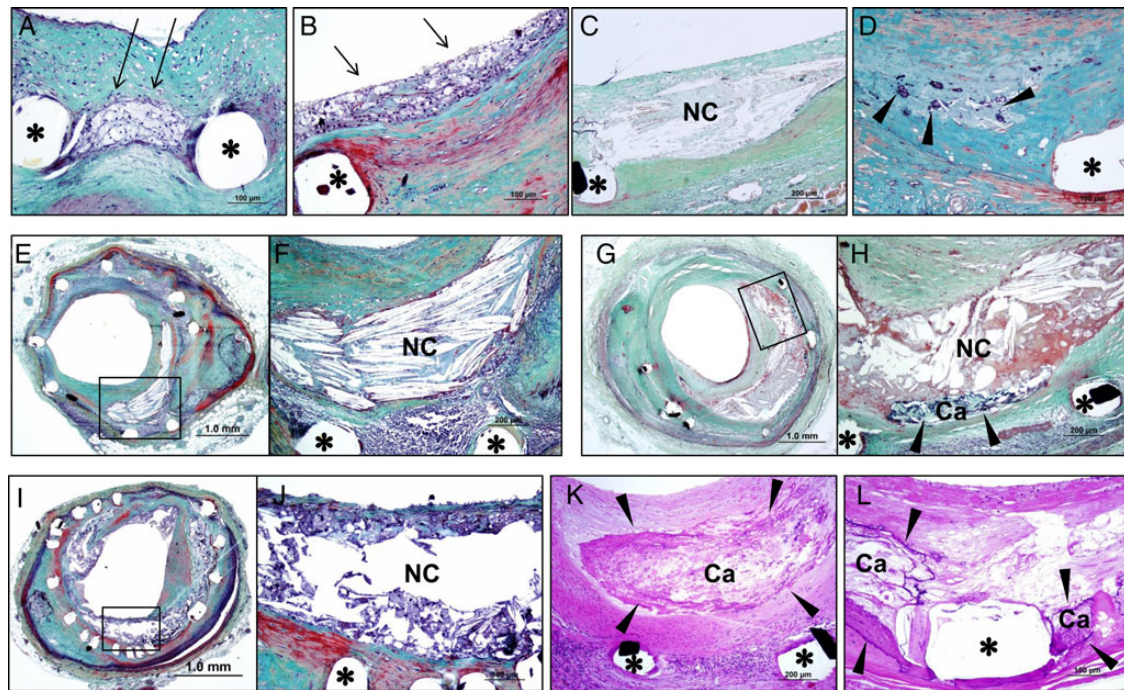
Figure 1 Representative histologic images showing progression of in-stent neoatherosclerosis. Foamy macrophage clusters in peri-strut region and close to the luminal surface in a sirolimus-eluting stent (A) and a paclitaxel-eluting stent (B). (C) Fibroatheroma showing necrotic core within thin neointima in a sirolimus-eluting stent. (D) Fibroatheroma with microcalcification (arrow heads) in a sirolimus-eluting stent. (E) and (F) are images at low- and high-power magnification of fibroatheroma within a bare metal stent (AVE stent). (G) and (H) are images of low- and high-power magnification of fibroatheroma with intra-plaque haemorrhage and fragmented calcification (Ca, arrow heads) within a sirolimus-eluting stent. (I) and (J) show low- and high-power magnified images of thin-cap fibroatheroma within a paclitaxel-eluting stent. (K) shows sheet calcification within a bare metal stent (NIR stent). Fragmented calcification is shown in (L) in peri-strut region of a paclitaxel-eluting stent. *Stent strut.

expression of ICAM-1 and VCAM-1 especially in peri-strut locations, which allows monocytes to adhere and migrate into the subendothelial space where they convert into macrophage-derived foam cells.[26,28,29] Early thrombus formation after stent implantation is a result of vascular injury, with fibrin and platelet deposition being an integral component of vascular healing. While thrombus generally resolves over time, there is persistence of fibrin in the peri-strut regions due to continued drug release and turbulent flow arising from non-streamlined stent struts.

Drug-eluting stent polymer coatings may also promote chronic inflammation characterized by infiltration of macrophages, lymphocyte, and giant cells,[30] which may contribute to the development of neoatherosclerosis. In addition, human autopsy analysis revealed that restenotic DES show greater proteoglycan deposition when compared with restenotic BMS, which may be a potential enhancer of neoatherosclerosis in DES, since extracellular matrix components such as proteoglycan are known to be associated with retention of lipoprotein.[31,32] Moreover, persistent apoptosis of macrophages and smooth muscle cells within the stented lesions further promote the development of necrotic core.[33,34] Pathologic intimal thickening with lipid pool is a hall mark of native atherosclerosis and plaque progression, whereas in neoatherosclerosis necrotic core formation is mostly driven by macrophage apoptosis in the

absence of lipid pool (Figure 2B), which eventually leads to in-stent plaque rupture (Figure 2C).

We have previously reported the presence of unstable underlying lesion morphology to be a significant risk factor for the formation of neoatherosclerosis following implantation of BMS and DES.[20] We hypothesize that DES implanted in unstable lesions may be prone to greater delay in vascular healing when compared with those implanted in stable lesions.[35] In unstable lesions, stent struts are embedded in the necrotic core, which is an avascular structure, where the effect of drug likely persists for a long period of time that potentially causes dysfunctional and/or incompetent endothelium, leading to the development of neoatherosclerosis. Also, it is possible that endothelial recovery is delayed owing to the absence of enough viable tissue required for arterial repair. We believe that the migration of underlying plaque into the neointima is an extremely unusual phenomenon in our cases as we carefully excluded lesions with direct communication between underlying atherosclerotic plaque and overlying neointima.

There remains a question whether neoatherosclerosis can be caused by plaque migration from the adjoining proximal and distal non-stented (stent edge) arterial segments. To determine the relationship of plaque progression from the adjacent non-stented arterial segments, we evaluated a total of 15 cases of in-stent plaque
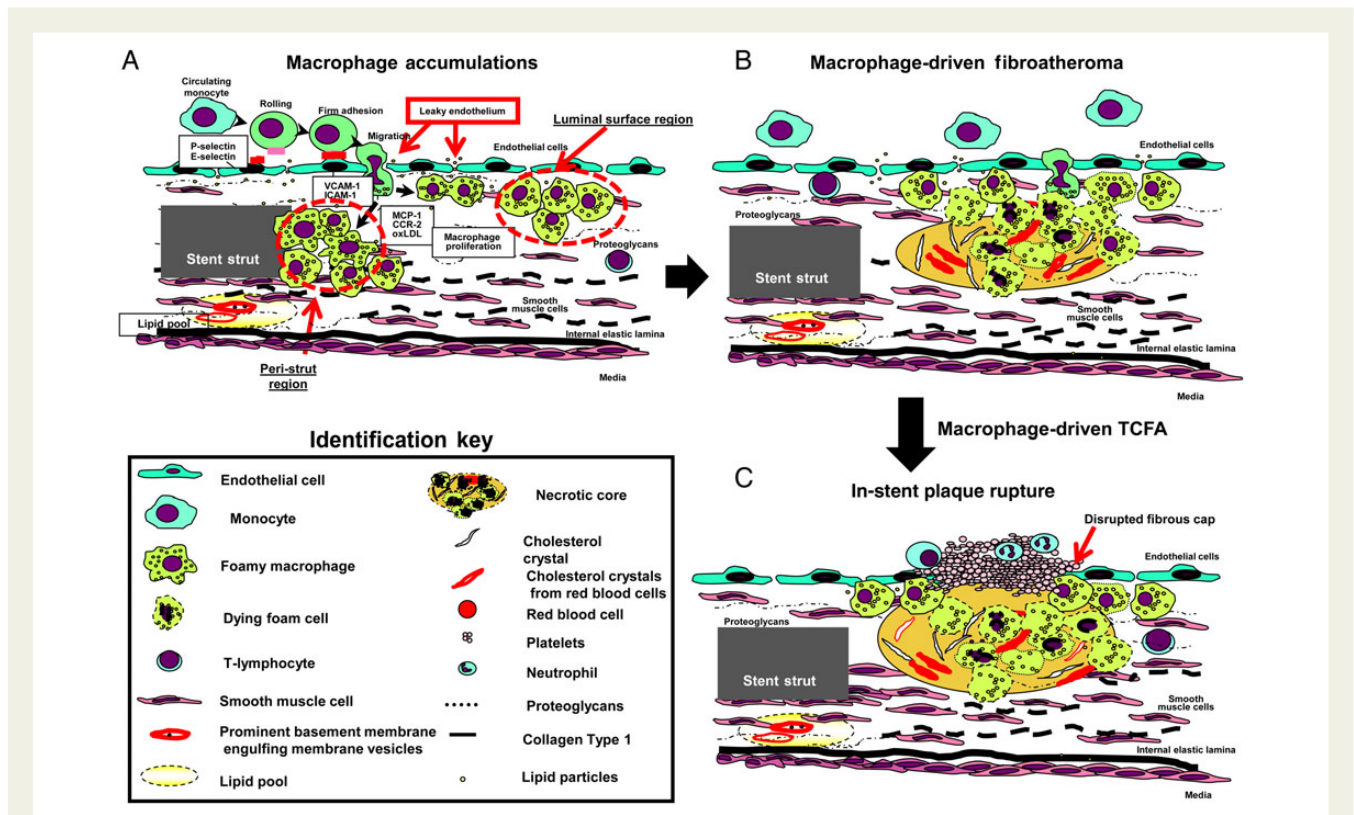
Figure 2 Schematic illustration showing potential mechanisms of the development of neoatherosclerosis. (*A*) Incompetent and dysfunctional endothelial coverage following stent placement particularly in drug-eluting stents characterized by poorly formed cell-to-cell junctions may allow greater entry of lipoproteins into the sub-endothelial space. Local blood flow disturbance following stent placement may also contribute to the continued activation of the regenerating endothelial cells towards a pro-inflammatory phenotype resulting in adhesion and migration of mono-cytes into the sub-endothelial space where they convert into foamy macrophages, either residing in the subluminal or peri-strut regions. Accu-mulation of proteoglycan within the neointima, especially following drug-eluting stents placement, may be associated with greater retention of lipoprotein to promote the development of neoatherosclerosis. (*B*) Accumulation of foamy macrophages and their persistent apoptosis likely results in the development of the necrotic core to form fibroatheroma. (*C*) Further enlargement of the necrotic core over time results in the formation of thin-cap fibroatheroma, which may eventually lead to in-stent plaque rupture.

rupture and/or in-stent TCFA with respect to their precise plaque location along the longitudinal axis from proximal or distal stent edges. The neoatherosclerotic lesions consisted of five TCFA in BMS, five ruptured plaques in BMS, two TCFA in DES, and three ruptured plaques in DES. Histologic sections were taken at 2−3 mm intervals to cover proximal non-stented, in-stent, and dis-tal non-stented segments, to assess the presence or absence of pla-que continuation from the non-stented to the stented arterial segments. Of these 15 cases, three showed presence of fibroather-oma (one proximal and two distal) in the adjacent arterial segments, and one had a TCFA in the distal stent edge, while the remaining 11 lesions did not show any plaques with necrotic core. Of these four lesions with necrotic core in the stent edges, three appeared to be in continuity with the in-stent neoatherosclerotic plaque (20%). Ob-servational intravascular ultrasound studies suggest plaque rupture occurs more frequently within the proximal and distal non-stented edge arterial segments resulting in complete or incomplete throm-botic occlusion of the stented artery.[36,37] While these early clinical observations suggest flow disturbances in the transition regions of

stented to native coronary artery, histopathological evaluation clearly shows that the majority of neoatherosclerotic plaques originate with-in the stented arterial segment and only infrequently are an extension from proximal or distal non-stented arterial segments.

Since plaque rupture is more likely to occur from superficial nec-rotic core, we sought to determine the location of the necrotic core in relationship to the thickness of neointimal growth. In our prelim-inary pathologic investigation involving a total of 23 neoathero-sclerotic lesions with fibroatheroma (6 BMS and 17 DES), superficial necrotic core (defined as within 200 µm from the luminal surface) was more frequently observed (17 lesions [4 BMS and 13 DES], 74%) when compared with deeper necrotic core (>200 µm) (6 lesions [2 BMS and 4 DES], 26%). It can therefore be concluded that the majority of fibroatheroma with necrotic core are located superficially. This may be related to suppression of smooth muscle cell proliferation within a thin neointimal layer in DES where foamy macrophages remain superficial and undergo apoptosis leading to necrotic core formation, which has been defined as 'graveyard of dead macrophages' by Ira Tabas.[38]

Prevalence of neoatherosclerosis in human autopsy analyses

A previous autopsy study conducted by our research group has demonstrated that the overall prevalence of neoatherosclerosis was significantly greater in lesions with first-generation DES (31%) when compared with BMS (16%), despite a longer duration of implant in the latter (*Figure 3A*).[20] In terms of the morphology of observed neoatherosclerosis, early features of neoatherosclerosis, i.e. foamy macrophage clusters, were seen more frequently in first-generation DES when compared with BMS (15 vs. 3%). In contrast, the prevalence of fibroatheroma and TCFA or in-stent plaque rupture was not significantly different between first-generation DES and BMS, despite substantial difference in duration of implant between the groups (*Figure 3A*). Importantly, the earliest time point at which foamy macrophage accumulation was observed was 70 days following PES and 120 days following SES implantation vs. at 900 days for BMS. Similarly, fibroatheroma with necrotic core formation was identified as early as 270 days after PES, 360 days after SES, and 900 days after BMS. Moreover, unstable features of neoatherosclerosis—i.e. TCFA and in-stent plaque rupture—were identified within 2 years following first-generation DES and 5 years following BMS placement.[20]

The prevalence of neoatherosclerosis in second-generation CoCr-EES (XIENCE V, Abbott Vascular, Santa Clara, CA, USA; or PROMUS, Boston Scientific) was recently reported by our group. We found no significant difference in the overall frequency of neoatherosclerosis between CoCr-EES and first-generation SES and PES with duration of implant >30 days and ≤3 years (CoCr-EES = 29%, SES = 35%, PES = 19%) (*Figure 3B*).[22] There was also no significant difference in the prevalence of neoatherosclerosis between the groups when divided into consecutive stages of plaque progression, although a dominant morphology in CoCr-EES and PES was foamy macrophage clusters (CoCr-EES = 67% [8 of 12]; PES = 87% [13 of 15]), which seemed to be less frequent in SES (32% [8 of 25]) (*Figure 3B*). The earliest duration of implant showing neoatherosclerosis in CoCr-EES was 270 days which was longer than SES and PES, and no unstable features of neoatherosclerosis were observed in CoCr-EES in this study population. The prevalence of neoatherosclerosis in E-ZES, Resolute-ZES (R-ZES; Medtronic), platinum-chromium EES (PtCr-EES; PROMUS Element, Boston Scientific), and biodegradable polymer-coated
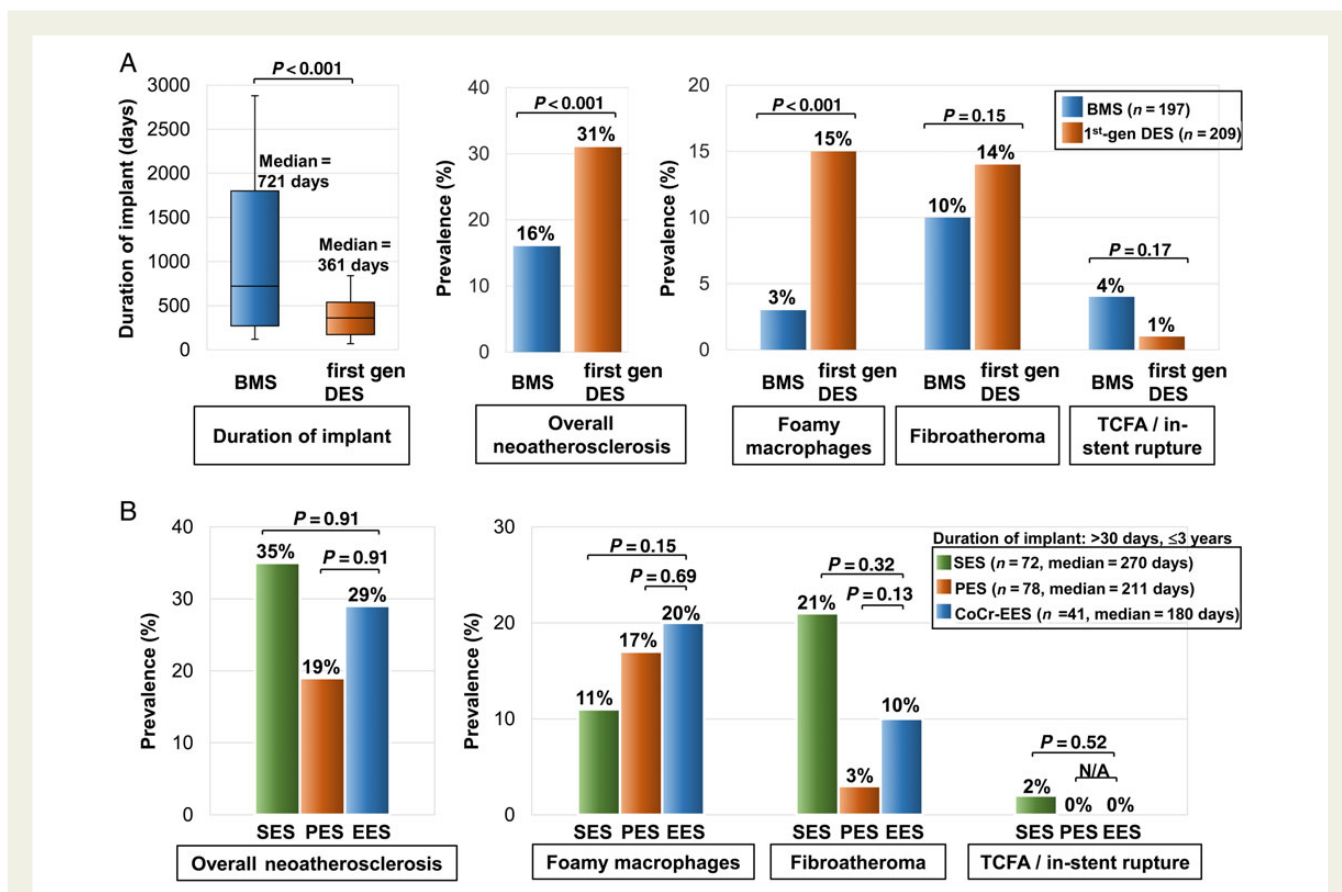

Figure 3 Prevalence and characteristics of neoatherosclerosis in human autopsy analyses. (*A*) Despite the shorter duration of implant in first-generation drug-eluting stents when compared with bare metal stent, first-generation drug-eluting stents showed greater prevalence of neoatherosclerosis, particularly those characterized by foamy macrophage clusters. (*B*) Observed frequency of neoatherosclerosis in second-generation cobalt-chromium everolimus-eluting stents was comparable with the first-generation sirolimus-eluting stent and paclitaxel-eluting stent. (*A*) is reproduced with permission from Ref.[20] and (*B*) is reproduced with permission from Ref.[22]
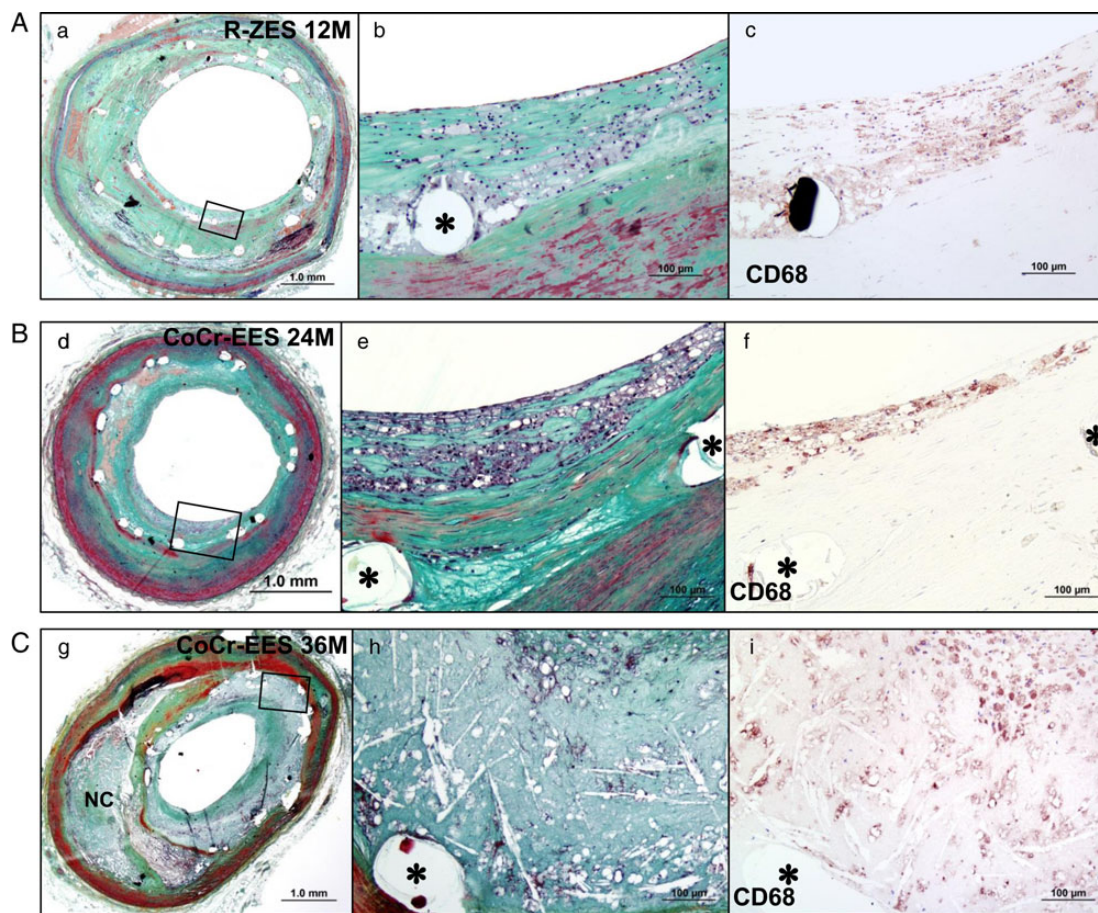
Figure 4 Representative histologic images showing neoatherosclerosis in second-generation drug-eluting stents. (*A*) Foamy macrophage clusters in Resolute zotarolimus-eluting stent. (*B*) Foamy macrophage accumulation in cobalt-chromium everolimus-eluting stents. (*C*) Fibroatheroma developed within cobalt-chromium everolimus-eluting stents. The presence of foamy macrophages was confirmed by immunostaining using an anti-CD68 antibody. *Stent strut. (*B*) and (*C*) are reproduced with permission from Ref.[22]

DES remains unclear because of limited availability of autopsy cases with these stents. Nevertheless, we have seen the development of neoatherosclerosis in R-ZES (*Figure 4*).

The prevalence of neoatherosclerosis was further evaluated according to the duration of implant using all available material with duration of implant >30 days (mean ± SD = 913 ± 989 days) from our autopsy stent registry. A total of 384 cases (mean age = 61 ± 13 years, 287 male) with 614 stented lesions in native coronary arteries, consisting of 266 lesions with BMS, 285 with first-generation DES (143 SES and 142 PES), and 63 with second-generation DES (7 E-ZES, 3 R-ZES, and 53 CoCr-EES) were histologically analysed (*Figure 5A*).[39] For duration of implant ≤1 year (n = 217 lesions), the prevalence of neoatherosclerosis was similar for the first-generation DES (13%) and second-generation DES (17%) but greater than BMS (0%). Similarly, for duration of implant >1 and ≤3 years (n = 218 lesions), neoatherosclerosis was similar for the first-generation DES (51%) and second-generation DES (48%) but greater than BMS (6%). For duration of implant >3 years (n = 179 lesions, no second-generation DES was available), the prevalence of neoatherosclerosis remained

greater for the first-generation DES (65%) when compared with BMS (38%) (*Figure 5A*). Thus, our autopsy analysis showed that first- and second-generation DES exhibit comparable prevalence of any neoatherosclerosis at least up to 3 years.

Neoatherosclerosis and late stent failure

In clinical practice, late stent failure—including LST/VLST and late in-stent restenosis—has emerged as an important issue following both BMS and DES implantation.[11,13,40,41] We sought to investigate whether neoatherosclerosis was associated with late stent failure. From our autopsy stent registry including all available 614 stented lesions in native coronary arteries, VLST from neoatherosclerosis (i.e. in-stent plaque rupture) was observed in 10 lesions (1.6%) (*Figure 6*).[39] Although the overall numbers are small, the prevalence of VLST from in-stent plaque rupture was similar between BMS (1.8% [5 of 285 lesions]) and first-generation DES (1.9% [5 of 266 lesions]) with none in second-generation DES, while duration
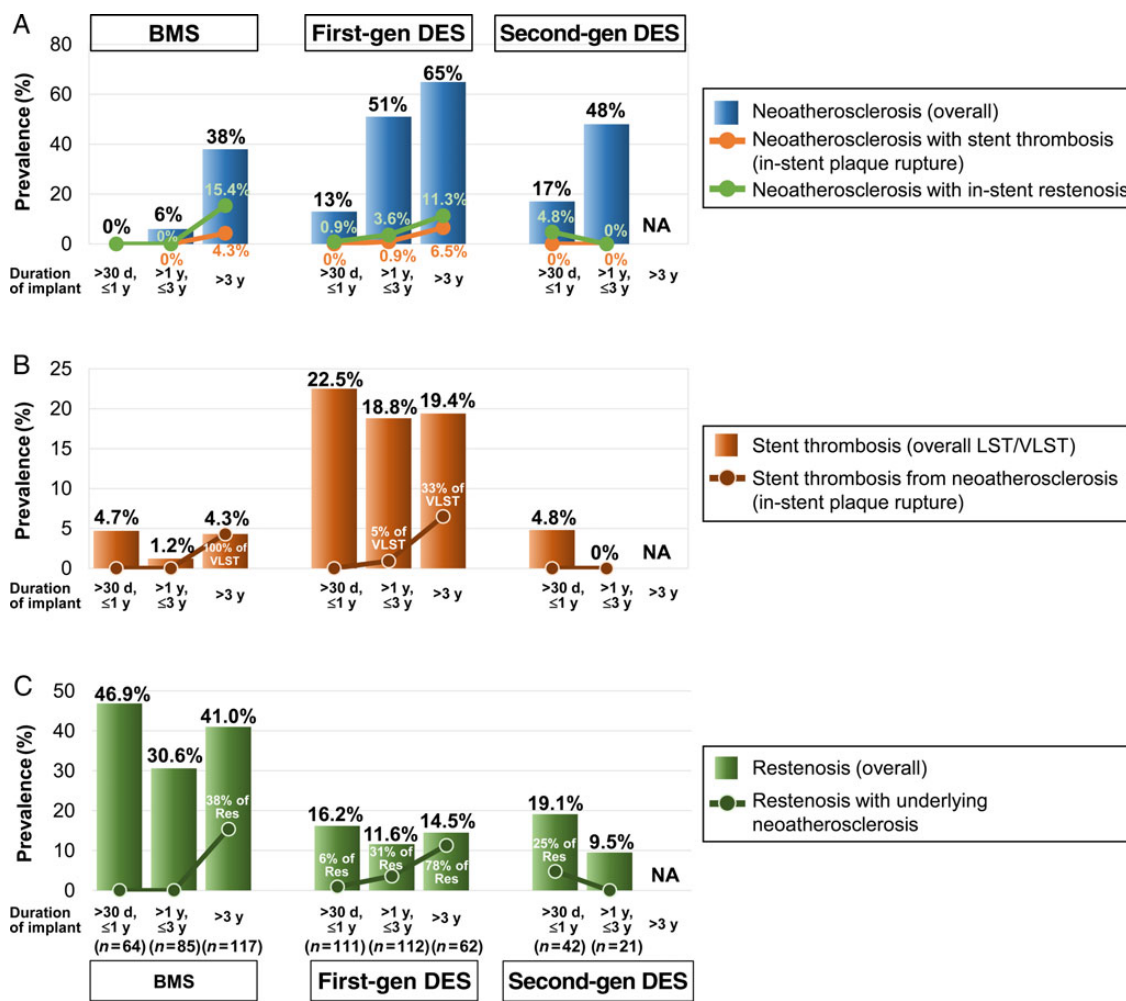
Figure 5 (A) Prevalence of neoatherosclerosis in bare metal stent, first- and second-generation drug-eluting stents stratified by duration of implant (bar graphs) along with the prevalence of restenosis (green line) and thrombosis (orange line) in the lesions with neoatherosclerosis and late stent failure. (B) Prevalence of overall stent thrombosis, in association with neoatherosclerosis (in-stent plaque rupture). (C) Prevalence of in-stent restenosis and its association with underlying neoatherosclerosis. LST/VLST, late and very late stent thrombosis; Res, restenosis.

of implant was significantly different among groups (median, BMS = 832 days, first-generation DES = 383 days, and second-generation DES = 210 days). Although the majority of neoatherosclerosis observed in our registry was classified as an incidental finding, the prevalence of VLST from in-stent plaque rupture increased with time in both BMS and first-generation DES (*Figure 5B*). Notably, the timing of VLST from in-stent plaque rupture was substantially earlier in first-generation DES when compared with BMS (*Figure 6E*). Of the 10 in-stent plaque ruptures, only four (three in BMS and one in first-generation DES) had in-stent restenosis (*Figure 6E*), highlighting that in-stent plaque rupture can occur from lesions with non-significant luminal narrowing, especially in DES.

The overall frequency of VLST (>1 year) due to any reason was 3.0% in BMS (6 of 202), 19% in first-generation DES (33 of 174), and none in second-generation DES (0 of 21). In-stent plaque rupture accounts for 83% of VLST in BMS (5 of 6) and 15% of VLST in

first-generation DES (5 of 33) in our autopsy stent registry. When we focused on stents with duration of implant beyond 3 years, all VLST in BMS (5 of 5) and 33% of VLST in first-generation DES (4 of 12) were attributed to in-stent plaque rupture (*Figure 5B*). The other cause of VLST (>1 year) in BMS was rupture of underlying vulnerable plaque at the proximal stent edge, whereas for first-generation DES, other aetiologies of VLST were uncovered struts associated with various conditions (penetration of stent struts into the necrotic core, overlapping stents, malapposition from excessive fibrin deposition, etc.) and hypersensitivity reaction, and least common cause was neointimal erosion.

Neointimal erosion is a relatively rare cause of VLST and is not necessarily associated with neoatherosclerosis (*Figure 7*). Although we have seen a case with VLST from neointimal erosion with underlying neoatherosclerosis (*Figure 7A*), it can occur without foamy macrophage accumulation or necrotic core formation, either in lesions with or without in-stent restenosis (*Figure 7B and C*).
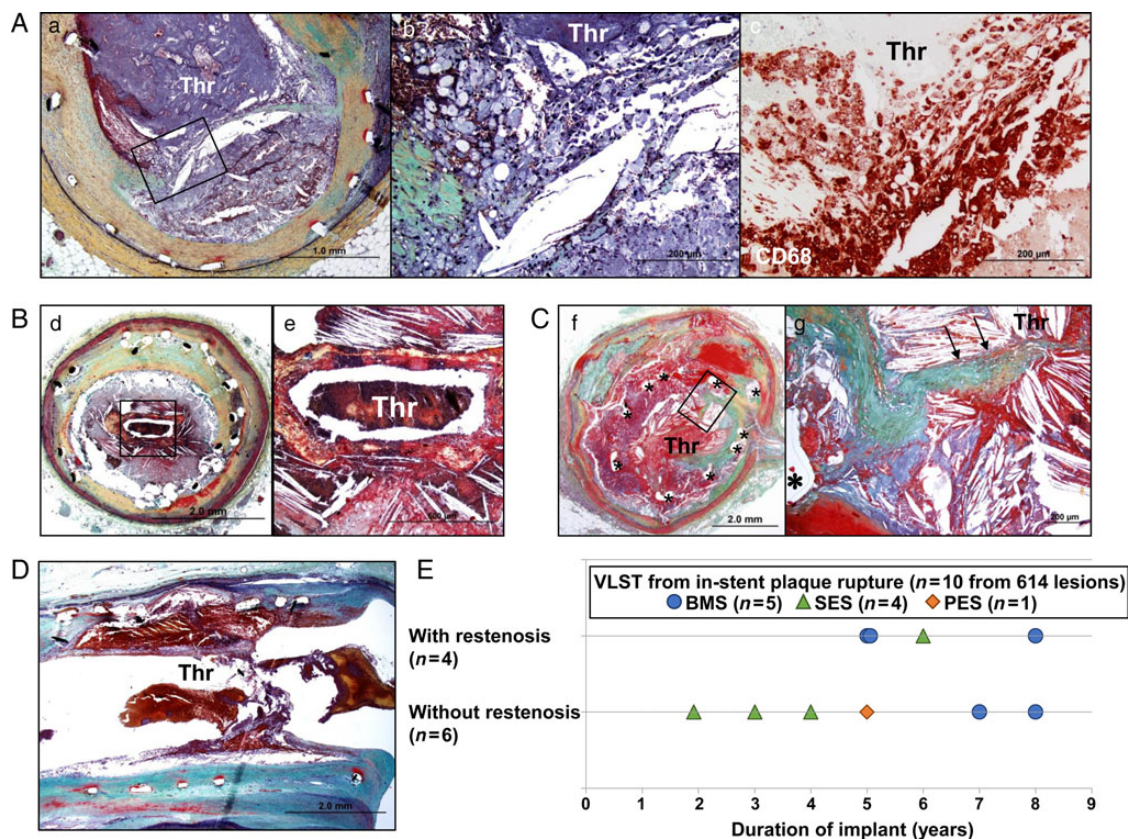
Figure 6 Very late stent thrombosis due to neoatherosclerosis with in-stent plaque rupture. (A) In-stent plaque rupture with luminal occlusive thrombus within bare metal stent (Gianturco-Roubin II stent) without restenosis. Large number of macrophages were identified at the ruptured cap by immunostaining using an anti-CD68 antibody (c). (B) In-stent plaque rupture in bare metal stent (two AVE) with restenosis. (C) In-stent plaque rupture within a sirolimus-eluting stent without restenosis. A fragment of disrupted fibrous cap (arrows) is visible in a high-power image (g). (D) Longitudinal histologic section showing in-stent plaque rupture within a bare metal stent (Mini-Crown) without restenosis. (E) Time distribution of 10 lesions with in-stent plaque rupture with or without in-stent restenosis in sirolimus-eluting stent, paclitaxel-eluting stent, and bare metal stent, obtained from all available 614 stented lesions in native coronary arteries in our autopsy registry. *Stent strut. (A), (B), and (D) are reproduced with permission from Ref.[20] and (C) is reproduced with permission from Ref.[26]

The contribution of neoatherosclerosis to the development of neointimal erosion remains unknown.

In-stent restenosis with underlying neoatherosclerosis was identified in 32 of 614 lesions (5.2%), and was most frequent in BMS (6.8% [18 of 266 lesions]) followed by first-generation DES (4.2% [12 of 285]), and was the least frequent in second-generation DES (3.2% [2 of 63]), while there was a substantial difference in duration of implant among the groups. In BMS, restenosis with neoatherosclerosis was exclusively observed beyond 3 years with a prevalence of 15.4% (Figure 5A), accounting for 38% of late restenosis in BMS beyond 3 years (18 of 48 lesions) (Figure 5C). On the other hand, restenosis with neoatherosclerosis in first-generation DES was observed at earlier time points and also increased with time (Figure 5A) similar to BMS. (11.3% ≤3 years, vs. 78% >3 years) (Figure 5C). For second-generation DES, restenosis with neoatherosclerosis was seen within 1 year but was not observed between 1 and 3 years (Figure 5A); nevertheless, further assessment with larger number of lesions with longer duration are needed.

While findings from our autopsy registry shows an association between neoatherosclerosis and in-stent restenosis (Figure 5A and C), a causative role of neoatherosclerosis per se in late restenosis formation cannot be established, since neoatherosclerosis may also occur late following development of restenosis within the neointimal hyperplasia. Nevertheless, accumulation of lipid and foamy macrophages are likely associated with increase in plaque burden, and it is likely that neoatherosclerosis contributes, at least partly, to the development of in-stent restenosis, especially in DES. Reminiscent of Glagov's phenomenon describing expansive remodelling during the early phase of progression of atherosclerotic plaques,[42] metallic stents constitute permanent scaffolds, which prohibit expansile remodelling and physiologic vasomotion. Therefore, incremental plaque growth will result in greater loss in lumen area, which upon exceeding a critical limit is likely to result in symptomatic or asymptomatic disease. As rapid progression of luminal narrowing in native coronary atherosclerosis is a hallmark of healed plaque rupture,[43] the same phenomenon may occur within neoatherosclerotic
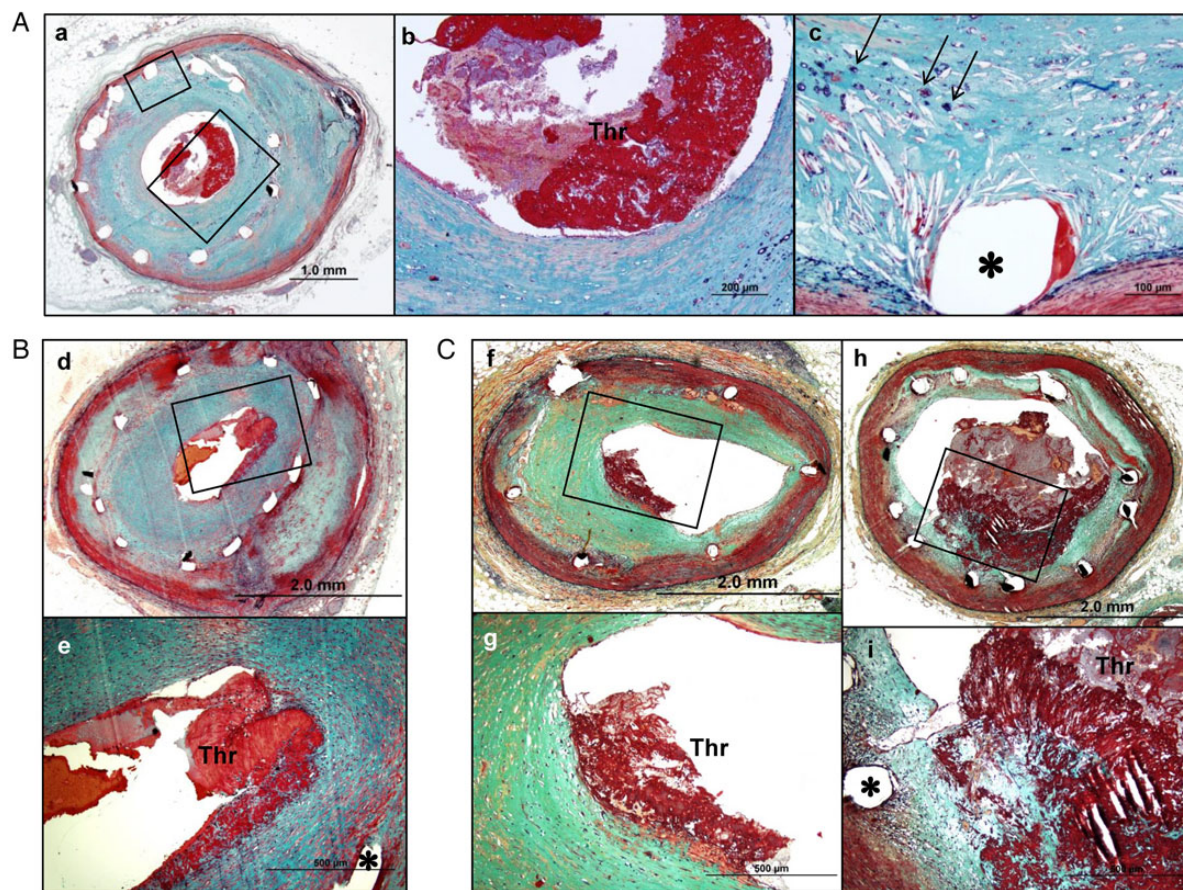
Figure 7 Late and very late stent thrombosis attributed to neointimal erosion with or without neoatherosclerosis. (A) Neointimal erosion with underlying neoatherosclerosis in a sirolimus-eluting stent implanted for 5 years. High-power images show acute platelet and fibrin-rich thrombus (b) and necrotic core formation with microcalcification (arrows) (c). (B) Neointimal erosion with in-stent restenosis without neoatherosclerosis in a bare metal stent (crown stent) implanted for 4 months. Note adherence of thrombus to the neointima. (C) Serial histologic sections (f and h) showing neointimal erosion without restenosis with no neoatherosclerosis in a sirolimus-eluting stent implanted for 2 years. Adherent thrombus is highlighted in high-power images in (g) and (i).

plaques in the stented segment. When VLST from in-stent plaque rupture may not manifest as acute coronary syndrome or sudden coronary death, in time the overlying thrombus will heal with inflammation, smooth muscle cell infiltration, and deposition of proteoglycans and collagen matrix, resulting in luminal narrowing and the development of in-stent restenosis. This process can also lead to occlusion, i.e. chronic total occlusion, although chronic total occlusion within the stents consists of organized thrombus and is not always derived from in-stent plaque rupture or restenosis.

Intravascular imaging of neoatherosclerosis

The prevalence and characteristics of in-stent neoatherosclerosis in living patients have been investigated by data acquired from intravascular imaging modalities, including angioscopy, intravascular ultrasound (IVUS), near-infrared spectroscopy, and optical coherence tomography (OCT) or optical frequency domain imaging (OFDI). Serial angioscopic studies have demonstrated that BMS show increase in yellow plaques from 4% at the first follow-up (6–12 months) to 58% at the second follow-up (4 years),[44] whereas in SES, 96% of the lesions (55 of 57) showed yellow plaques at 10 months, of which 17 lesions (30%) had white neointima at baseline and turned into yellow plaques within 10 months.[45] A virtual histology IVUS assessment of restenotic neointimal tissue in BMS ($n = 47$, mean = 43.5 months) and DES ($n = 70$, mean = 11.1 months) revealed that duration of implant correlated positively with percent necrotic core ($r = 0.35$) and percent dense calcium ($r = 0.57$), providing further evidence that the prevalence of neoatherosclerosis increases with time both in BMS and DES.[46] However, findings from IVUS-based tissue characterization should be interpreted with caution because the technology lacks sufficient resolution (spatial resolution = 150–250 μm) to enable reliable determination of plaque composition.

Optical coherence tomography or optical frequency domain imaging has superior axial resolution (10–20 μm) enabling better characterization of neointimal tissue within stents. Takano et al.[47]

evaluated neointimal characteristics following BMS placement by OCT at early (<6 months) and late (≥5 years) phases; lipid-laden neointima was exclusively observed at late phase: in 67% (14 of 21) patients, of whom 12 patients (86%) had in-stent restenosis. Habara et al.[48] compared neointimal characteristics between early (≤1 year) and late restenosis within BMS (>5 years, no restenosis ≤1 year) by OCT, and showed that heterogeneous-appearance of neointima was more frequent in late restenosis (61%) when compared with early restenosis (6%). Moreover, Kang et al.[49] investigated 50 patients who presented with stable (n = 30) or unstable angina (n = 20) with DES restenosis by OCT (median duration of implant = 32.2 months) and found lipid-containing neointima in 90% of lesions. Twenty-six

lesions (52%) had TCFA-containing neointima and 29 lesions (58%) had at least one in-stent neointimal rupture. Clinical predictors of neoatherosclerosis as detected by OCT have been further reported by Yonetsu et al.,[50] who assessed 179 stents (mean duration = 26.9 months, DES = 59%) with mean neointimal thickness >100 μm and reported OCT-detected neoatherosclerosis (lipid-laden neointima and/or calcification within the neointima) in 84 lesions (47%). Multivariate analysis demonstrated that longer duration of implant (≥48 months), DES usage, current smoking, chronic kidney disease, and an absence of angiotensin-converting enzyme inhibitors or angiotensin II receptor blockade usage were independent determinants of OCT-detected neoatherosclerosis.[50]
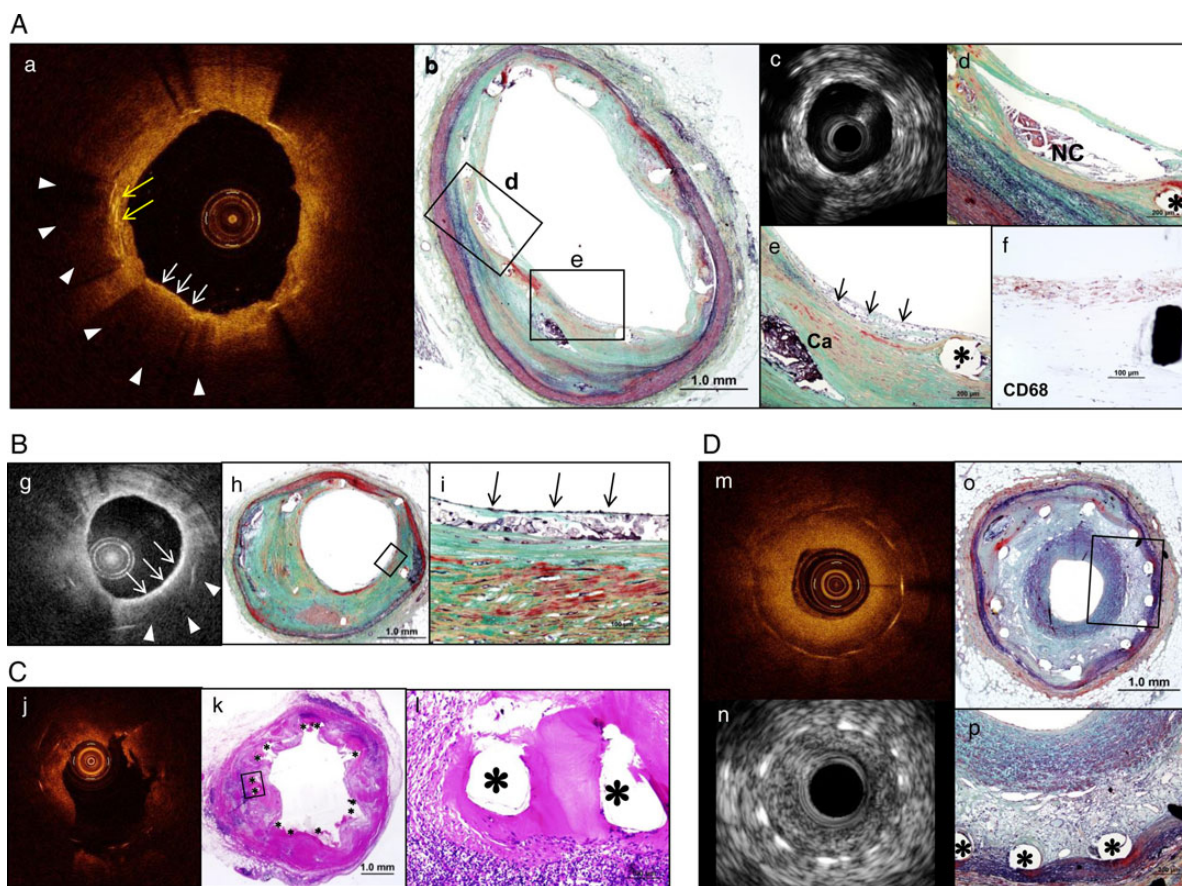

Figure 8 *Ex vivo* intravascular imaging with corresponding histologic sections showing stented coronary lesions with (*A* and *B*) and without (*C* and *D*) neoatherosclerosis. (a), (j), and (m) show optical coherence tomography images and (g) shows an optical frequency domain imaging image, while (c) and (n) show intravascular ultrasound images. (*A* and *B*) Neoatherosclerosis characterized by foamy macrophage accumulation can be detected by optical coherence tomography/optical frequency domain imaging as a thin bright signal (white arrows in [a] and [g]) with a trailing shadow (i.e. signal attenuation; white arrowheads in [a] and [g]). Linear, highly backscattering region (yellow arrows in [a]) with attenuation (white arrowheads in [a]) indicates the presence of cholesterol crystals in the necrotic core. The presence of superficial foamy macrophages (e and i) was confirmed by immunostaining using anti-CD68 antibody (f). Note the presence of fragmented calcification behind the superficial foamy macrophages in (e), which cannot be detected by optical coherence tomography in (a). (*C*) Hypersensitivity reaction in a sirolimus-eluting stent. Optical coherence tomography shows signal poor region in the deeper neointima (j) and histology demonstrated extensive inflammation predominantly consisting of eosinophils and T-lymphocytes with excessive fibrin deposition around stent struts (malapposition) (k and l). (*D*) Signal poor region without attenuation in the deeper intima as assessed by optical coherence tomography (m). The corresponding histologic images (o and p) show granulation tissue consisting of extracellular matrix and angiogenesis with varying degree of inflammatory cells. (*B*) is reproduced with permission from Ref.[51]
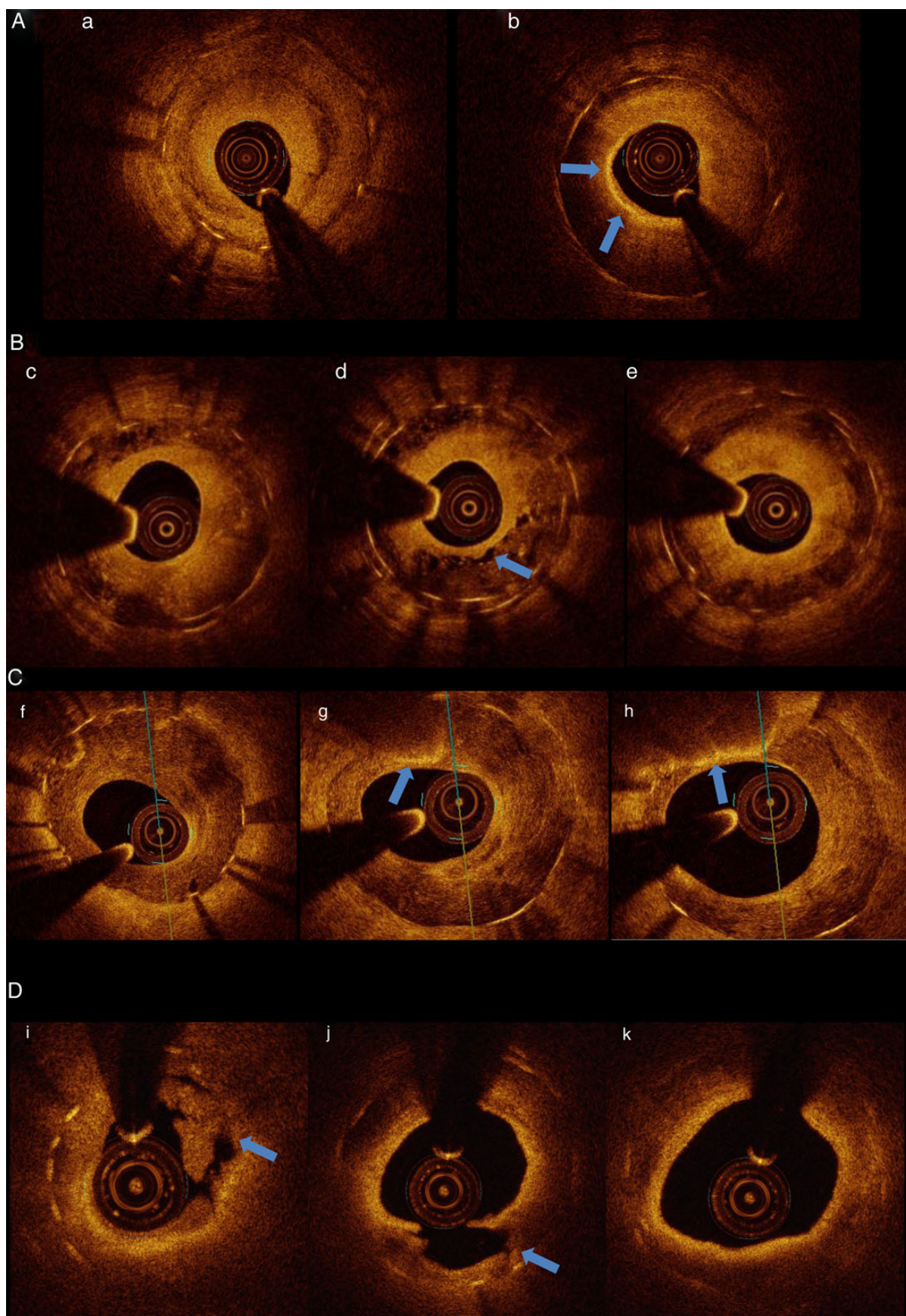
It is noteworthy that the prevalence of neoatherosclerosis in clinical OCT studies[47,49] appears to be greater than that observed in our autopsy stent registry (*Figures 3* and *5*). For instance, the prevalence of neoatherosclerosis in first-generation DES with restenosis beyond 3 years was 78% (7 of 9 lesions) at autopsy, where TCFA was identified in only 11% (1 of 9 lesions); against this in a study with clinical OCT assessment of DES restenosis showing TCFA-containing neointima in 52%.[49] Although direct comparison of data sets must be undertaken with caution due to a substantial difference in study population between clinical OCT studies and human autopsy analysis, there appears to be discordance between the prevalence of neoatherosclerosis found in autopsy cases and that observed in OCT-studies. This reflects concern regarding the potential over-diagnosis of neoatherosclerosis by OCT.

Ex vivo correlation of human coronary arteries by OCT/OFDI and histology demonstrated that neoatherosclerosis characterized by foamy macrophage accumulation can be detected by OCT as a thin bright signal with a trailing shadow, which is similar to what has been reported in native coronary arteries (*Figure 8A* and *B*).[51,52] However, the presence of foamy macrophages on the luminal surface as detected by OCT, along with an artefact called 'tangential signal dropout', can mask a TCFA and therefore need to be carefully interpreted.[53] Necrotic core can be detected by OCT as high attenuation signal poor region with poorly defined borders, which may or may not be accompanied by a linear, high backscattering region suggestive of cholesterol crystals and macrophages (*Figure 8A*).[51,52] However, it should be recognized that signal poor areas in OCT imaging are not exclusively caused by necrotic core. Indeed, we have noted that fibrin accumulation also appears as signal poor region without clear borders, which is mostly observed around stent struts (especially in PES) but is also seen in hypersensitivity reaction characterized by diffuse circumferential inflammation predominantly consisting of T-lymphocytes and eosinophils (*Figure 8C*).[51] Another possible cause of signal poor areas

within the neointima on OCT imaging is granulation tissue or organized thrombus consisting of extracellular matrix and angiogenesis with varying degrees of inflammatory cell infiltrate, which is diffusely or focally seen in the deep neointima around stent struts (*Figure 8D*). Moreover, the presence of lipid pool, which is observed in early progressive lesions termed pathologic intimal thickening, can also be detected by OCT as signal poor region with indiscriminant borders that is similar to the necrotic core.[52]

Thus, we contend that the complex features of neointimal tissues detected by OCT cannot be fully differentiated (*Figure 9A−D*). The limitations of tissue characterization with this technology need to be taken into account in the diagnosis of neoatherosclerosis in clinical studies. Perhaps, combination-imaging modalities may allow a more accurate detection of neoatherosclerosis. While a number of clinical imaging studies have compared the findings of intravascular imaging and histology in the past, there is a paucity of prospectively designed imaging studies applying pre-defined criteria for the distinction of various atherosclerotic plaque morphologies providing comprehensive validation prior to human use. In the absence of such studies, there will always remain a level of uncertainty that will prohibit successful translation of intravascular imaging modalities for the prediction of cardiovascular events.

Clinical perspectives

In view of their demonstrated high efficacy and safety out to 5 years, DES are now dominant devices used in PCI and have been implanted in millions of patients world wide. Nevertheless, the development of accelerated neoatherosclerosis within DES,[20] even with newer-generation DES,[22] raises potential concerns regarding safety and efficacy over the longer term. This may have an important impact on public health and costs related to future treatments. Moreover, although the mechanisms of late stent failure are likely multifactorial, the development of neoatherosclerosis increases with time and

Figure 9 Clinical assessment of stented coronary arteries by optical coherence tomography showing variety of neointimal tissues. (*A*) A 55-year-old male patient presented with unstable angina 9 years after left anterior descending artery stenting with a durable polymer paclitaxel-eluting stent. Optical coherence tomography imaging revealed diffuse high-grade in-stent restenosis of the stented segment. Cross-sectional analysis of the distal stented segment (a) shows homogeneous high signal intensity close to the luminal surface with signal poor region in the middle of the neointima. This may be represent neointimal hyperplasia with smooth muscle cell growth and accumulation of lipid or extracellular matrix such as proteoglycan, or healed lesion secondary to thrombotic event. The proximal stented segment (b) shows an area of plaque with superficial high signal intensity (arrows), which may represent foamy macrophages accumulation. Deep to this, there is high signal attenuation which may indicates granulation tissue or the accumulation of lipid or fibrin. (*B*) Focal recurrent in-stent restenosis 4 years after durable polymer sirolimus-eluting stent implantation for in-stent restenosis in the proximal right coronary artery (RCA). Optical coherence tomography imaging confirmed focal restenosis with otherwise satisfactory result in the stented segment. Cross-sectional images of the restenotic area show heterogeneous and layered pattern tissue (c−e). The relatively well-demarcated borders and the lack of signal attenuation (d) suggest that this is unlikely to represent lipid-rich neoatherosclerosis but is likely granulation tissue with overlying neointimal hyperplasia rich in smooth muscle cells. Focal areas of signal dropout (arrow in d) likely represent neovascularization. (*C*) A 58-year-old male patient presented with stable angina 7 months after implantation of a durable polymer everolimus-eluting stent. Optical coherence tomography imaging showed focal in-stent restenosis. Cross-sectional analysis shows heterogeneous signal intensity in the neointima with relatively low attenuation (f−h). Such appearances may represent proteoglycan-rich neointima but another possibility includes granulation tissue or fibrin deposition. The middle (g) and the proximal (h) sections show focal signal rich region with attenuation (arrows) that indicate neoatherosclerosis characterized by foamy macrophage clusters. (*D*) A 67-year-old patient presented with stent thrombosis in the RCA 3 years after implantation of a durable polymer drug-eluting stents. Optical coherence tomography imaging after thrombus aspiration revealed generally good healing of the proximal stented segment. The distal stented segment showed moderate concentric restenosis with signal rich region close to the luminal surface accompanied by signal attenuation (obscuring stent struts) (i−k) with evidence of plaque rupture (arrow in j). The most-distal stented segment (i) shows high-grade eccentric restenosis with residual intraluminal thrombus (arrow in i). These appearances indicate that the stent thrombosis was attributed to in-stent plaque rupture from neoatherosclerosis.

therefore the contribution of neoatherosclerosis to late stent failure is likely significant. The factors that predispose individuals to neoatherosclerosis, and their overlap with risk factors for native atherosclerosis, remain poorly defined, and effective treatment strategies to prevent this complication have yet to be established. Future studies are needed to identify patients at risk of developing neoatherosclerosis after stent implantation. Longitudinal follow-up studies employing one or more intravascular imaging methodologies in the presence or absence of disease-modifying approaches such as high dose statin usage are warranted to study the true prevalence and therapeutic approaches to further understand neoatherosclerosis in clinical practice.

In the short-term, improved algorithms and characterization of neoatherosclerosis are of utmost importance as reliable diagnosis of neoatherosclerosis is key to evaluating the effects of any disease-modifying therapy. If incompetent re-generated endothelium plays a pivotal role in the development of neoatherosclerosis, evaluation of competent strut coverage will also be important. Various methods for molecular imaging, such as combined fluorescence and OCT probe using a double-clad fibre combiner[54] or near-infrared fluorescence imaging with indocyanine green administration,[55] may enable more accurate detection of atherosclerotic lesions within the stented segment, though application for routine clinical usage remains unproven.

Limitations

Optical coherence tomography and histopathology utilize different sampling intervals, where OCT provides a more or less continuous reflection of the arterial morphology, while histopathological cross-sections in the current study were taken at 2–3 mm intervals, which introduces potential under-appreciation of the presence and extent of neoatherosclerotic lesions by histology. Nevertheless, very focal lesions with longitudinal dimension of <2–3 mm are extremely rare and should have been captured with the currently applied histopathological sampling technique.

Conclusions

Data from autopsy registries and clinical imaging studies suggest that in-stent neoatherosclerosis is a clinically important disease entity in patients undergoing coronary stenting. Evidence to date implicates neoatherosclerosis in both VLST and in-stent restenosis. Moreover, its incidence appears to be accelerated after implantation of first- and second-generation DES in comparison with BMS. In addition, as the prevalence increases with time in both DES and BMS, neoatherosclerosis likely plays an important role in stent failure occurring at longer durations after stent implantation. The introduction of OCT has facilitated detection of neoatherosclerosis in clinical practice. However, tissue morphology within stents is complex and correlation data with histopathology remains small. In our experience, differentiation of neoatherosclerosis from other types of in-stent tissue can be challenging. Description of detailed histopathologic features of neoatherosclerosis in the current review, along with discussion of the limitations of current intravascular imaging technologies, may facilitate better interpretation of acquired imaging data in clinical practice. Further refinement of imaging acquisition

and analysis protocols will be required to more accurately characterize neoatherosclerosis, and to permit the investigation of targeted anti-atherosclerotic therapies to prevent neoatherosclerosis-associated late stent failure and to improve patient outcomes.

References

1. Mieres JH. Review of the American Heart Association's guidelines for cardiovascular disease prevention in women. *Heart* 2006;**92** (Suppl. 3):iii10–13.
2. Go AS, Mozaffarian D, Roger VL, Benjamin EJ, Berry JD, Blaha MJ, Dai S, Ford ES, Fox CS, Franco S, Fullerton HJ, Gillespie C, Hailpern SM, Heit JA, Howard VJ, Huffman MD, Judd SE, Kissela BM, Kittner SJ, Lackland DT, Lichtman JH, Lisabeth LD, Mackey RH, Magid DJ, Marcus GM, Marelli A, Matchar DB, McGuire DK, Mohler ER III, Moy CS, Mussolino ME, Neumar RW, Nichol G, Pandey DK, Paynter NP, Reeves MJ, Sorlie PD, Stein J, Towfighi A, Turan TN, Virani SS, Wong ND, Woo D, Turner MB. Heart disease and stroke statistics – 2014 update: a report from the American Heart Association. *Circulation* 2014; **129**:e28–e292.
3. Grines CL, Browne KF, Marco J, Rothbaum D, Stone GW, O'Keefe J, Overlie P, Donohue B, Chelliah N, Timmis GC, Vlietstra RE, Strzelecki M, Puchrowicz-Ochocki S, O'Neill WW; the Primary Angioplasty in Myocardial Infarction Study Group. A comparison of immediate angioplasty with thrombolytic therapy for acute myocardial infarction. The Primary Angioplasty in Myocardial Infarction Study Group. *N Engl J Med* 1993;**328**:673–679.
4. Cannon CP, Weintraub WS, Demopoulos LA, Vicari R, Frey MJ, Lakkis N, Neumann FJ, Robertson DH, DeLucca PT, DiBattiste PM, Gibson CM, Braunwald E. Comparison of early invasive and conservative strategies in patients with unstable coronary syndromes treated with the glycoprotein IIb/IIIa inhibitor tirofiban. *N Engl J Med* 2001;**344**:1879–1887.
5. Morice MC, Serruys PW, Sousa JE, Fajadet J, Ban Hayashi E, Perin M, Colombo A, Schuler G, Barragan P, Guagliumi G, Molnar F, Falotico R. A randomized comparison of a sirolimus-eluting stent with a standard stent for coronary revascularization. *N Engl J Med* 2002;**346**:1773–1780.
6. Joner M, Finn AV, Farb A, Mont EK, Kolodgie FD, Ladich E, Kutys R, Skorija K, Gold HK, Virmani R. Pathology of drug-eluting stents in humans: delayed healing and late thrombotic risk. *J Am Coll Cardiol* 2006;**48**:193–202.
7. Kimura T, Morimoto T, Nakagawa Y, Kawai K, Miyazaki S, Muramatsu T, Shiode N, Namura M, Sone T, Oshima S, Nishikawa H, Hiasa Y, Hayashi Y, Nobuyoshi M, Mitudo K. Very late stent thrombosis and late target lesion revascularization after sirolimus-eluting stent implantation: five-year outcome of the j-Cypher Registry. *Circulation* 2012;**125**:584–591.
8. Tada T, Byrne RA, Simunovic I, King LA, Cassese S, Joner M, Fusaro M, Schneider S, Schulz S, Ibrahim T, Ott I, Massberg S, Laugwitz KL, Kastrati A. Risk of stent thrombosis among bare-metal stents, first-generation drug-eluting stents, and second-

generation drug-eluting stents: results from a registry of 18,334 patients. *JACC Cardiovasc Interv* 2013;**6**:1267–1274.

9. Raber L, Magro M, Stefanini GG, Kalesan B, van Domburg RT, Onuma Y, Wenaweser P, Daemen J, Meier B, Juni P, Serruys PW, Windecker S. Very late coronary stent thrombosis of a newer-generation everolimus-eluting stent compared with early-generation drug-eluting stents: a prospective cohort study. *Circulation* 2012;**125**:1110–1121.

10. Daemen J, Wenaweser P, Tsuchida K, Abrecht L, Vaina S, Morger C, Kukreja N, Juni P, Sianos G, Hellige G, van Domburg RT, Hess OM, Boersma E, Meier B, Windecker S, Serruys PW. Early and late coronary stent thrombosis of sirolimus-eluting and paclitaxel-eluting stents in routine clinical practice: data from a large two-institutional cohort study. *Lancet* 2007;**369**:667–678.

11. Wenaweser P, Daemen J, Zwahlen M, van Domburg R, Juni P, Vaina S, Hellige G, Tsuchida K, Morger C, Boersma E, Kukreja N, Meier B, Serruys PW, Windecker S. Incidence and correlates of drug-eluting stent thrombosis in routine clinical practice. 4-year results from a large 2-institutional cohort study. *J Am Coll Cardiol* 2008;**52**:1134–1140.

12. Cassese S, Byrne RA, Tada T, Pinieck S, Joner M, Ibrahim T, King LA, Fusaro M, Laugwitz KL, Kastrati A. Incidence and predictors of restenosis after coronary stenting in 10 004 patients with surveillance angiography. *Heart* 2014;**100**:153–159.

13. Natsuaki M, Morimoto T, Furukawa Y, Nakagawa Y, Kadota K, Yamaji K, Ando K, Shizuta S, Shiomi H, Tada T, Tazaki J, Kato Y, Hayano M, Abe M, Tamura T, Shirotani M, Miki S, Matsuda M, Takahashi M, Ishii K, Tanaka M, Aoyama T, Doi O, Hattori R, Kato M, Suwa S, Takizawa A, Takatsu Y, Shinoda E, Eizawa H, Takeda T, Lee JD, Inoko M, Ogawa H, Hamasaki S, Horie M, Nohara R, Kambara H, Fujiwara H, Mitsudo K, Nobuyoshi M, Kita T, Kimura T. Late adverse events after implantation of sirolimus-eluting stent and bare-metal stent: long-term (5–7 years) follow-up of the coronary revascularization demonstrating outcome study-kyoto registry cohort-2. *Circ Cardiovasc Interv* 2014;**7**:168–179.

14. Brener SJ, Kereiakes DJ, Simonton CA, Rizvi A, Newman W, Mastali K, Wang JC, Caputo R, Smith RS Jr, Ying SW, Cutlip DE, Stone GW. Everolimus-eluting stents in patients undergoing percutaneous coronary intervention: final 3-year results of the Clinical Evaluation of the XIENCE V Everolimus Eluting Coronary Stent System in the treatment of subjects with de novo native coronary artery lesions trial. *Am Heart J* 2013;**166**:1035–1042.

15. Lee JM, Park KW, Han JK, Yang HM, Kang HJ, Koo BK, Bae JW, Woo SI, Park JS, Jin DK, Jeon DW, Oh SK, Kim DI, Hyon MS, Jeon HK, Lim DS, Kim MG, Rha SW, Her SH, Hwang JY, Kim S, Choi YJ, Kang JH, Moon KW, Jang Y, Kim HS. Three-year patient-related and stent-related outcomes of second-generation everolimus-eluting Xience V stents versus zotarolimus-eluting resolute stents in real-world practice (from the Multicenter Prospective EXCELLENT and RESOLUTE-Korea Registries). *Am J Cardiol* 2014;**114**:1329–1338.

16. Camenzind E, Wijns W, Mauri L, Kurowski V, Parikh K, Gao R, Bode C, Greenwood JP, Boersma E, Vranckx P, McFadden E, Serruys PW, O'Neil WW, Jorissen B, Van Leeuwen F, Steg PG. Stent thrombosis and major clinical events at 3 years after zotarolimus-eluting or sirolimus-eluting coronary stent implantation: a randomised, multicentre, open-label, controlled trial. *Lancet* 2012;**380**:1396–1405.

17. Finn AV, Joner M, Nakazawa G, Kolodgie F, Newell J, John MC, Gold HK, Virmani R. Pathological correlates of late drug-eluting stent thrombosis: strut coverage as a marker of endothelialization. *Circulation* 2007;**115**:2435–2441.

18. Nakazawa G, Finn AV, Vorpahl M, Ladich ER, Kolodgie FD, Virmani R. Coronary responses and differential mechanisms of late stent thrombosis attributed to first-generation sirolimus- and paclitaxel-eluting stents. *J Am Coll Cardiol* 2011;**57**:390–398.

19. Nakazawa G, Finn AV, Vorpahl M, Ladich E, Kutys R, Balazs I, Kolodgie FD, Virmani R. Incidence and predictors of drug-eluting stent fracture in human coronary artery a pathologic analysis. *J Am Coll Cardiol* 2009;**54**:1924–1931.

20. Nakazawa G, Otsuka F, Nakano M, Vorpahl M, Yazdani SK, Ladich E, Kolodgie FD, Finn AV, Virmani R. The pathology of neoatherosclerosis in human coronary implants: bare-metal and drug-eluting stents. *J Am Coll Cardiol* 2011;**57**:1314–1322.

21. Nakazawa G, Vorpahl M, Finn AV, Narula J, Virmani R. One step forward and two steps back with drug-eluting-stents: from preventing restenosis to causing late thrombosis and nouveau atherosclerosis. *JACC Cardiovasc Imaging* 2009;**2**:625–628.

22. Otsuka F, Vorpahl M, Nakano M, Foerst J, Newell JB, Sakakura K, Kutys R, Ladich E, Finn AV, Kolodgie FD, Virmani R. Pathology of second-generation everolimus-eluting stents versus first-generation sirolimus- and Paclitaxel-eluting stents in humans. *Circulation* 2014;**129**:211–223.

23. Otsuka F, Sakakura K, Yahagi K, Joner M, Virmani R. Has our understanding of calcification in human coronary atherosclerosis progressed? *Arterioscler Thromb Vasc Biol* 2014;**34**:724–736.

24. Joner M, Nakazawa G, Finn AV, Quee SC, Coleman L, Acampado E, Wilson PS, Skorija K, Cheng Q, Xu X, Gold HK, Kolodgie FD, Virmani R. Endothelial cell recovery between comparator polymer-based drug-eluting stents. *J Am Coll Cardiol* 2008;**52**:333–342.

25. Nakazawa G, Nakano M, Otsuka F, Wilcox JN, Melder R, Pruitt S, Kolodgie FD, Virmani R. Evaluation of polymer-based comparator drug-eluting stents using a rabbit model of iliac artery atherosclerosis. *Circ Cardiovasc Interv* 2011;**4**:38–46.

26. Otsuka F, Finn AV, Yazdani SK, Nakano M, Kolodgie FD, Virmani R. The importance of the endothelium in atherothrombosis and coronary stenting. *Nat Rev Cardiol* 2012;**9**:439–453.

27. Guagliumi G, Farb A, Musumeci G, Valsecchi O, Tespili M, Motta T, Virmani R. Images in cardiovascular medicine. Sirolimus-eluting stent implanted in human coronary artery for 16 months: pathological findings. *Circulation* 2003;**107**:1340–1341.

28. Jimenez JM, Davies PF. Hemodynamically driven stent strut design. *Ann Biomed Eng* 2009;**37**:1483–1494.

29. Davies PF. Hemodynamic shear stress and the endothelium in cardiovascular pathophysiology. *Nat Clin Pract Cardiovasc Med* 2009;**6**:16–26.

30. Nakazawa G, Ladich E, Finn AV, Virmani R. Pathophysiology of vascular healing and stent mediated arterial injury. *EuroIntervention* 2008;**4 Suppl C**:C7–10.

31. Nakano M, Otsuka F, Yahagi K, Sakakura K, Kutys R, Ladich ER, Finn AV, Kolodgie FD, Virmani R. Human autopsy study of drug-eluting stents restenosis: histomorphological predictors and neointimal characteristics. *Eur Heart J* 2013;**34**:3304–3313.

32. Williams KJ, Tabas I. The response-to-retention hypothesis of early atherogenesis. *Arterioscler Thromb Vasc Biol* 1995;**15**:551–561.

33. Tabas I. Consequences and therapeutic implications of macrophage apoptosis in atherosclerosis: the importance of lesion stage and phagocytic efficiency. *Arterioscler Thromb Vasc Biol* 2005;**25**:2255–2264.

34. Tulenko TN, Chen M, Mason PE, Mason RP. Physical effects of cholesterol on arterial smooth muscle membranes: evidence of immiscible cholesterol domains and alterations in bilayer width during atherogenesis. *J Lipid Res* 1998;**39**:947–956.

35. Nakazawa G, Finn AV, Joner M, Ladich E, Kutys R, Mont EK, Gold HK, Burke AP, Kolodgie FD, Virmani R. Delayed arterial healing and increased late stent thrombosis at culprit sites after drug-eluting stent placement for acute myocardial infarction patients: an autopsy study. *Circulation* 2008;**118**:1138–1145.

36. Wakabayashi K, Mintz GS, Weissman NJ, Stone GW, Ellis SG, Grube E, Ormiston JA, Turco MA, Pakala R, Xue Z, Desale S, Laynez-Carnicero A, Romaguera R, Sardi G, Pichard AD, Waksman R. Impact of drug-eluting stents on distal vessels. *Circ Cardiovasc Interv* 2012;**5**:211–219.

37. Wakabayashi K, Waksman R, Weissman NJ. Edge effect from drug-eluting stents as assessed with serial intravascular ultrasound: a systematic review. *Circ Cardiovasc Interv* 2012;**5**:305–311.

38. Thorp E, Tabas I. Mechanisms and consequences of efferocytosis in advanced atherosclerosis. *J Leukoc Biol* 2009;**86**:1089–1095.

39. Otsuka F, Sakakura K, Yahagi K, Sanchez OD, Kutys B, Ladich E, Fowler DR, Kolodgie FD, Davis HR, Joner M, Virmani R. Contribution of in-stent neoatherosclerosis to late stent failure following bare metal and 1st- and 2nd-generation drug-eluting stent placement: an autopsy study. *J Am Coll Cardiol* 2014;**64**(11 Suppl.):B190–B191.

40. Yamaji K, Kimura T, Morimoto T, Nakagawa Y, Inoue K, Soga Y, Arita T, Shirai S, Ando K, Kondo K, Sakai K, Goya M, Iwabuchi M, Yokoi H, Nosaka H, Nobuyoshi M. Very long-term (15 to 20 years) clinical and angiographic outcome after coronary bare metal stent implantation. *Circ Cardiovasc Interv* 2010;**3**:468–475.

41. Doyle B, Rihal CS, O'Sullivan CJ, Lennon RJ, Wiste HJ, Bell M, Bresnahan J, Holmes DR Jr. Outcomes of stent thrombosis and restenosis during extended follow-up of patients treated with bare-metal coronary stents. *Circulation* 2007;**116**:2391–2398.

42. Glagov S, Weisenberg E, Zarins CK, Stankunavicius R, Kolettis GJ. Compensatory enlargement of human atherosclerotic coronary arteries. *N Engl J Med* 1987;**316**:1371–1375.

43. Burke AP, Kolodgie FD, Farb A, Weber DK, Malcom GT, Smialek J, Virmani R. Healed plaque ruptures and sudden coronary death: evidence that subclinical rupture has a role in plaque progression. *Circulation* 2001;**103**:934–940.

44. Yokoyama S, Takano M, Yamamoto M, Inami S, Sakai S, Okamatsu K, Okuni S, Seimiya K, Murakami D, Ohba T, Uemura R, Seino Y, Hata N, Mizuno K. Extended follow-up by serial angioscopic observation for bare-metal stents in native coronary arteries: from healing response to atherosclerotic transformation of neointima. *Circ Cardiovasc Interv* 2009;**2**:205–212.

45. Higo T, Ueda Y, Oyabu J, Okada K, Nishio M, Hirata A, Kashiwase K, Ogasawara N, Hirotani S, Kodama K. Atherosclerotic and thrombogenic neointima formed over sirolimus drug-eluting stent: an angioscopic study. *JACC Cardiovasc Imaging* 2009;**2**:616–624.

46. Kang SJ, Mintz GS, Park DW, Lee SW, Kim YH, Lee CW, Han KH, Kim JJ, Park SW, Park SJ. Tissue characterization of in-stent neointima using intravascular ultrasound radiofrequency data analysis. *Am J Cardiol* 2010;**106**:1561–1565.

47. Takano M, Yamamoto M, Inami S, Murakami D, Ohba T, Seino Y, Mizuno K. Appearance of lipid-laden intima and neovascularization after implantation of bare-metal stents extended late-phase observation by intracoronary optical coherence tomography. *J Am Coll Cardiol* 2009;**55**:26–32.

48. Habara M, Terashima M, Nasu K, Kaneda H, Inoue K, Ito T, Kamikawa S, Kurita T, Tanaka N, Kimura M, Kinoshita Y, Tsuchikane E, Matsuo H, Ueno K, Katoh O, Suzuki T. Difference of tissue characteristics between early and very late restenosis lesions after bare-metal stent implantation: an optical coherence tomography study. *Circ Cardiovasc Interv* 2011;**4**:232–238.

49. Kang SJ, Mintz GS, Akasaka T, Park DW, Lee JY, Kim WJ, Lee SW, Kim YH, Whan Lee C, Park SW, Park SJ. Optical coherence tomographic analysis of in-stent neoatherosclerosis after drug-eluting stent implantation. *Circulation* 2011;**123**: 2954–2963.

50. Yonetsu T, Kato K, Kim SJ, Xing L, Jia H, McNulty I, Lee H, Zhang S, Uemura S, Jang Y, Kang SJ, Park SJ, Lee S, Yu B, Kakuta T, Jang IK. Predictors for neoatherosclerosis: a retrospective observational study from the optical coherence tomography registry. *Circ Cardiovasc Imaging* 2012;**5**:660–666.

51. Nakano M, Vorpahl M, Otsuka F, Taniwaki M, Yazdani SK, Finn AV, Ladich ER, Kolodgie FD, Virmani R. Ex vivo assessment of vascular response to coronary stents by optical frequency domain imaging. *JACC Cardiovasc Imaging* 2012;**5**:71–82.

52. Otsuka F, Joner M, Prati F, Virmani R, Narula J. Clinical classification of plaque morphology in coronary disease. *Nat Rev Cardiol* 2014;**11**:379–389.

53. van Soest G, Regar E, Goderie TP, Gonzalo N, Koljenovic S, van Leenders GJ, Serruys PW, van der Steen AF. Pitfalls in plaque characterization by OCT: image artifacts in native coronary arteries. *JACC Cardiovasc Imaging* 2011;**4**: 810–813.

54. Liang S, Saidi A, Jing J, Liu G, Li J, Zhang J, Sun C, Narula J, Chen Z. Intravascular atherosclerotic imaging with combined fluorescence and optical coherence tomography probe based on a double-clad fiber combiner. *J Biomed Opt* 2012; **17**:070501.

55. Vinegoni C, Botnaru I, Aikawa E, Calfon MA, Iwamoto Y, Folco EJ, Ntziachristos V, Weissleder R, Libby P, Jaffer FA. Indocyanine green enables near-infrared fluorescence imaging of lipid-rich, inflamed atherosclerotic plaques. *Sci Transl Med* 2011;**3**: 84ra45.